

Interference of integrated Floquet-Bloch waves

P. St. J. Russell

IBM Thomas J. Watson Research Center, P.O. Box 218, Yorktown Heights, New York 10598

(Received 16 September 1985)

The interference of scalar optical Floquet-Bloch waves in periodically stratified media is discussed in detail. Two main types of interference are identified and fully analyzed: normal and exchange interference, producing, respectively, real and virtual spatial fringes. In the paper considerable use is made of a reciprocal-space representation of the Floquet-Bloch waves (the wave-vector diagram), first introduced in the dynamical theory of x-ray diffraction. Experimental observations of the interference of integrated versions of the Floquet-Bloch waves, made in corrugated planar Ta₂O₅ waveguides, are included by way of illustration.

I. INTRODUCTION

The simplest electromagnetic disturbances that can exist in a periodically stratified medium are the Floquet-Bloch waves.^{1,2} These waves consist of stable periodic amplitude distributions transverse to the stratifications, progressing in phase along them, with group velocities pointing at some angle to them. Their group velocities yield the directions of the rays of the Floquet-Bloch waves, which play the same role as do the rays of conventional optics in isotropic media. Thus one can imagine a Floquet-Bloch ray getting reflected and refracted at an interface, the incident energy being carried off in the rays of the reflected and refracted Floquet-Bloch waves. There is little published work in which Floquet-Bloch wave analogies of effects well known and understood in conventional optics are discussed. In this paper one such effect is singled out for treatment—interference. In contrast to the interference of plane waves in isotropic media, it turns out that the Floquet-Bloch waves can interfere in two distinct ways, one resulting in a redistribution of energy in *real* space, the other in a redistribution of energy in *reciprocal* space. The first produces real (i.e., visible) fringes of the conventional type, and the second virtual fringes that produce no redistribution of energy in real space, but instead affect its angular distribution, energy getting *exchanged* between two groups of spectral plane waves traveling in phase in directions parallel to the upper and lower first-order Bragg angles. These two types of interference I shall call respectively *normal* and *exchange* interference, labels made necessary by the fact that this is the first time such a distinction has been made. Two-dimensional *integrated* Floquet-Bloch waves can be observed directly in the light scattered (due to ever-present cosmetic imperfections) from corrugated planar waveguides.^{3,4} The truly two-dimensional nature of such waveguides allows the observation of many effects predicted (but not easily confirmed experimentally) by the dynamical theory of x-ray diffraction in crystals. That theory^{5,6} provides a natural basis for the discussion in this paper, although my preoccupations are rather different since corrugated planar waveguides can be fabricated to order, unlike crystalline materials. Some photographs confirming the existence of

normal and exchange interference between these integrated Floquet-Bloch waves are presented and interpreted. In the course of the discussion, the roles of the Poynting vector and the group velocity are clarified, as they have an important bearing on the interference of the Floquet-Bloch waves.

II. THE INTERFERENCE OF TWO PLANE WAVES

As a starting point, I consider the interference of two monochromatic plane waves in an isotropic lossless medium. This is in order to clarify the roles played by group velocity, Poynting vector, and phase velocity. As is well known, the dispersion relation for the eigenmodes in this kind of medium (the plane waves) takes the form

$$f(\omega, \mathbf{k}) = (\omega/c)^2 N^2 - \mathbf{k}^2 = (k_v N)^2 - \mathbf{k}^2 = 0, \quad (1)$$

where ω is the optical angular frequency, \mathbf{k} the wave vector, N the refractive index, c the velocity of light *in vacuo*, and $k_v = \omega/c$. The group velocity \mathbf{v}_g follows directly from the dispersion relation. One takes the gradient of ω in wave-vector space:

$$\mathbf{v}_g = \nabla_{\mathbf{k}} \omega(\mathbf{k}) = (c/N) \hat{\mathbf{k}}, \quad (2)$$

where $\hat{\mathbf{k}}$ is a unit vector parallel to \mathbf{k} . One can thus only speak sensibly of the group velocity of a single plane wave (eigenmode), and of course it points parallel to the wave vector \mathbf{k} . A complex field consisting of a linear superposition of n plane waves will have n independent group velocities. However, the Poynting vector of this set of superimposed plane waves *is* affected by interference. For example, consider the case of two scalar plane waves

$$\mathbf{E}(\mathbf{r}) = \sum_{m=-1}^0 A_m \hat{\mathbf{z}} \exp(-j\mathbf{k}_m \cdot \mathbf{r}). \quad (3)$$

Their time-averaged Poynting vector takes the form

$$\begin{aligned} \langle \mathbf{S} \rangle = & \frac{1}{2\omega\mu} (A_0^2 \mathbf{k}_0 + A_{-1}^2 \mathbf{k}_{-1} \\ & + \{2A_0 A_{-1} k_v N \cos\theta \cos[(\mathbf{k}_0 - \mathbf{k}_{-1}) \cdot \mathbf{r}]\} \hat{\mathbf{x}}), \end{aligned} \quad (4)$$

where the amplitudes A_0 and A_{-1} have been taken to be real variables, and θ is half the angle between the two wave vectors. This Poynting vector can be resolved into components parallel and perpendicular to the fringes, in the x and y directions, respectively. It might appear at first glance that the amount of energy carried by the combination fluctuates across the interference fringes, suggesting that power is not conserved. However, the Poynting vector tells us that only the x component of $\langle \mathbf{S} \rangle$ is spatially modulated, indicating that power is merely *redistributed* in real space. The y component of $\langle \mathbf{S} \rangle$ (crossing the fringes) is spatially constant, equal to zero if the two waves have equal amplitudes.

III. THE FLOQUET-BLOCH WAVES

Before launching into a discussion of the interference of the Floquet-Bloch waves, one needs a clear physical picture of what these waves are, and how they behave. I consider a lossless dielectric medium in which the propagation constant β is modulated periodically, with a strength M and a spatial period Λ ($=2\pi/|\mathbf{K}|$ where \mathbf{K} is the grating vector):

$$\beta^2(\mathbf{r}) = k_v^2 N^2 [1 + M \cos(\mathbf{K} \cdot \mathbf{r})]. \quad (5)$$

A Floquet-Bloch wave (or eigenmode) in this medium consists of a complex, transverse, periodic amplitude distribution (period equal to the spacing of the stratifications) that progresses at a constant phase velocity parallel to the stratifications, and travels (in the direction of its group velocity) at some angle to them. Its field can be described in terms of an infinite set of interfering spectral plane waves chosen such that the resulting fringe pattern has a fundamental spatial frequency of Λ . This is in effect the Floquet-Bloch theorem. To ensure that this requirement always holds, the wave vectors of the participating spectral plane waves have to take the form

$$\mathbf{k}_n = \mathbf{k}_0 + n\mathbf{K}, \quad (6)$$

where \mathbf{k}_n is the wave vector of the n th spectral wave. In the simplest case, the field itself can be described quite accurately in terms of just two of these spectral waves (this yields a sinusoidal transverse distribution, in the so-called two-wave approximation), and the scalar Floquet-Bloch field (polarized in the z direction) is then

$$E(\mathbf{r}) = \sum_{n=-1}^0 V_n \exp(-j\mathbf{k}_n \cdot \mathbf{r}) = a(y) \exp(-jk_{0x}x), \quad (7)$$

where V_n is the amplitude of the n th spectral wave, and k_{0x} the x component of \mathbf{k}_0 . Notice that the Floquet-Bloch wave can also be written as a transverse periodic distribution $a(y)$ across the grating, with a phase velocity ω/k_{0x} in the x direction along the grating lines. Putting Eq. (7) into the scalar wave equation

$$[\nabla^2 + \beta^2(\mathbf{r})]E = 0 \quad (8)$$

and setting the coefficients of like exponentials to zero, the following matrix equation is obtained:

$$\begin{bmatrix} (k_v N)^2 - \mathbf{k}_0^2 & M(k_v N)^2/2 \\ M(k_v N)^2/2 & (k_v N)^2 - \mathbf{k}_{-1}^2 \end{bmatrix} \begin{bmatrix} V_0 \\ V_{-1} \end{bmatrix} = \begin{bmatrix} 0 \\ 0 \end{bmatrix}. \quad (9)$$

The dispersion relation follows straightforwardly by setting the determinant of coefficients equal to zero. In terms of spatial dispersion, we then have the loci in wave-vector space of \mathbf{k}_0 (and hence \mathbf{k}_{-1}) at fixed optical frequency ω . For $M=0$, any value of \mathbf{k}_0 (or \mathbf{k}_{-1}) is allowed provided its modulus equals $k_v N$, but nonzero accompanying values of V_{-1} (or V_0) can appear *only* if \mathbf{k}_0 (or \mathbf{k}_{-1}) points exactly in one discrete direction. This direction defines the Bragg condition,

$$\sin\theta_B = (K/2k_v N) = (\lambda_{\text{eff}}/2\Lambda), \quad (10)$$

where λ_{eff} is the effective mean wavelength of light in the stratified medium. The two associated *Lorentz points* (borrowing a term from x-ray theorists⁵) in wave-vector space have the position vectors

$$\bar{\mathbf{k}}_{LP_n} = \{ \hat{\mathbf{x}}[(k_v N)^2 - (K/2)^2]^{1/2} + \hat{\mathbf{y}}K(1+2n)/2 \}, \quad n=0, -1 \quad (11)$$

where $\hat{\mathbf{x}}$ and $\hat{\mathbf{y}}$ are unit vectors, respectively, normal and parallel to \mathbf{K} , and the bar signifies that the wave vector can exist only when $M=0$.

For $M=0$ the situation in wave-vector space is depicted in Fig. 1, where the fundamental circle $\mathbf{k}_0^2 = (k_v N)^2$ is drawn with a solid line, and the higher-order circles

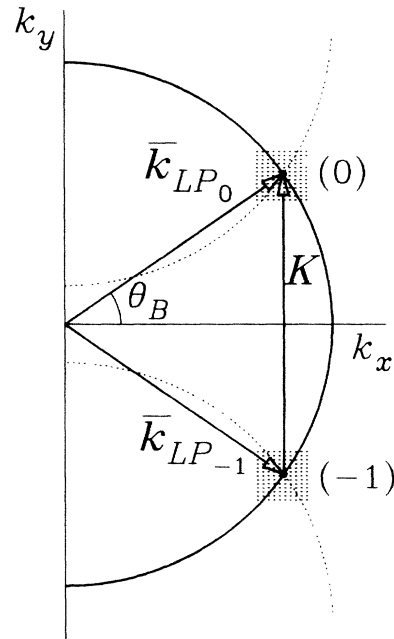


FIG. 1. Plot of the wave-vector diagram for positive values of k_x (the grating lines lie parallel to the x axis in real space). The wave vector \mathbf{k}_0 is defined as having a positive k_y component, and \mathbf{k}_{-1} as having a negative. For zero grating strength ($M=0$), the only two waves that can coexist with nonzero amplitudes, at the same time satisfying the Floquet condition in Eq. (6), are those whose wave vectors satisfy the Bragg condition as shown in the figure. The points (0) and (-1) thus defined are called the *Lorentz points*.

$\mathbf{k}_n = \mathbf{k}_0 + n\mathbf{K}$ (of which because of the finite size of the diagram only two are to be seen, those for $n = \pm 1$) are drawn with dashed lines. By Floquet's theorem, the wave vectors of all the spectral plane waves [given by Eq. (6) for all values of n], are required for consistency, even though in the two-wave approximation only two of their associated amplitudes (V_0 and V_{-1}) are non-negligible.

For $M > 0$, the points where both V_0 and V_{-1} are nonzero expand into *regions* of wave-vector space, and *stop bands* form around the Lorentz points. To evaluate the shape of the stop-band branches, we shall define a new set of axes (ξ, η) with its origin at the upper Lorentz point [given by $n = 0$ in Eq. (11)]. Putting

$$\mathbf{k}_n = \bar{\mathbf{k}}_{LPn} + \xi \hat{\mathbf{x}} + \eta \hat{\mathbf{y}} \quad (12)$$

into the determinant from Eq. (9) and neglecting terms of order higher than 2 in $\xi/k_v N$ and $\eta/k_v N$, the locus of the stop band (see Fig. 2) takes the form

$$(2\xi/w_{SB})^2 = 1 + (2\eta \tan\theta_B/w_{SB})^2, \quad (13)$$

where w_{SB} is the minimum stop-band width, given by

$$w_{SB} = M k_v N / 2 \cos\theta_B = 2\kappa / \cos\theta_B \quad (14)$$

and κ is the coupling constant of coupled-wave theory.⁷ This is the equation of a pair of hyperbolas with asymptotes at $\eta = \pm \xi \cot\theta_B$; these asymptotes are the theory's approximation to the two circles that intersect at the Lorentz points in Fig. 1. It can be seen that the size of the interaction region in the vicinity of the Lorentz point (which scales with the stop-band width) depends directly on the grating strength M .

The group velocity⁸ of any particular Floquet-Bloch wave follows from the dispersion relation as in Eq. (2):

$$\mathbf{v}_g = \nabla_{\mathbf{k}} \omega(\mathbf{k}_0).$$

It points normal to the stop-band branches, and can therefore lie anywhere between $\pm\theta_B$ (compare Figs. 1 and 2). A straightforward analysis [with the same approximations as those used to obtain Eq. (13)] yields

$$\mathbf{v}_g = (c/N) [\hat{\mathbf{x}} \cos\theta_B - \hat{\mathbf{y}} (\eta^\dagger/\xi^\dagger) \sin\theta_B], \quad (15)$$

where the normalized coordinates η^\dagger and ξ^\dagger are defined by

$$\begin{aligned} \eta^\dagger &= 2\eta \tan\theta_B / w_{SB}, \\ \xi^\dagger &= 2\xi / w_{SB}. \end{aligned} \quad (16)$$

From Eq. (15), the angle α which the group velocity

$$\langle \mathbf{S} \rangle = \left(\frac{1}{2}\right) \text{Re}(\mathbf{E} \times \mathbf{H}^*)$$

$$= (E_0^2 N^2 / 2\mu c^2) (\mathbf{v}_g \pm (c/N) \{ \hat{\mathbf{x}} \cos\theta_B [1 - (\tan\alpha / \tan\theta_B)^2]^{1/2} \} \cos(\mathbf{K} \cdot \mathbf{r})). \quad (19)$$

The x component of $\langle \mathbf{S} \rangle$ is spatially modulated with a period Λ . Power is redistributed spatially, just as was the case for the two plane waves discussed in Sec. II. In fact, the Poynting vectors in the two cases are identical in form. One cannot tell from Eq. (19) whether we are deal-

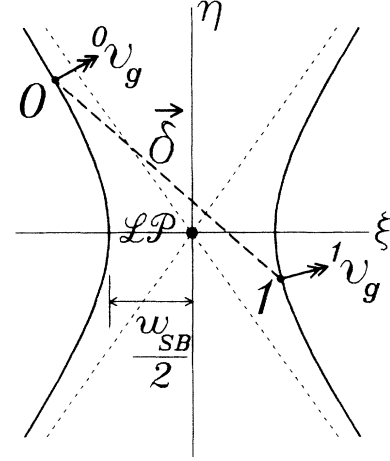


FIG. 2. Magnified drawing of one of the shaded regions in Fig. 1 for nonzero grating strength. The crossing dotted lines represent the intersecting circles, and the solid lines the locus of solutions of the dispersion relation. The tie points labeled 0 and 1 yield a difference wave vector δ which defines the spacing and orientation of the interference fringes created by the two associated Floquet-Bloch waves, whose group velocities are given by the double-headed arrows.

makes with the x axis (i.e., with the grating lines) is

$$\alpha = \arctan[-(\eta^\dagger/\xi^\dagger) \tan\theta_B]. \quad (17)$$

The normalized mode shape $\{\mathbf{V}\}$ of this Floquet-Bloch wave is

$$\begin{bmatrix} V_0 \\ V_{-1} \end{bmatrix} = \frac{1}{\sqrt{2}} \begin{bmatrix} +[1 - (\eta^\dagger/\xi^\dagger)]^{1/2} \\ \pm[1 + (\eta^\dagger/\xi^\dagger)]^{1/2} \end{bmatrix}, \quad (18)$$

where the plus sign refers to a Floquet-Bloch wave with a "tie point" (i.e., its position on one of the stop-band branches) on the right-hand branch, and the minus sign to one with a tie point on the left-hand branch. Tie points on the left-hand branch yield Floquet-Bloch waves with faster phase velocities along the grating lines compared to those on the right-hand branch. I shall therefore designate these two types of Floquet-Bloch waves as *fast* and *slow*. $\{\mathbf{V}\}$ is real-valued provided $|\xi^\dagger| > 1$, a condition that holds for traveling Floquet-Bloch waves, i.e., ones for which \mathbf{k}_0 is real-valued. Scaling this dimensionless modal shape with an electric field E_0 , the time-averaged Poynting vector of the Floquet-Bloch wave is

ing with a pair of independent plane waves in an isotropic medium or with a Floquet-Bloch wave. Only by looking at the group velocity is the fundamental difference apparent. If the Poynting vector is averaged over a grating period, the oscillatory term in Eq. (19) vanishes, and the

resulting vector $\langle \mathbf{S}_{av} \rangle$ points parallel to the group velocity. The group of spectral plane waves constituting the Floquet-Bloch wave travels *not* in an oscillatory path as one might be tempted to suspect from Eq. (19), *but in the direction of the group velocity*. A single Floquet-Bloch wave has an angular spectrum containing two δ functions in the directions of \mathbf{k}_0 and \mathbf{k}_{-1} ; if the energy carried by these spectral delta functions is spread out over a finite angular range, then in real space one will see a finite Floquet-Bloch beam traveling in (and diffracting about) the direction of its central group velocity, *not* parallel to either of the now quasiplane spectral waves.

Notice that as $\alpha \rightarrow \pm\theta_B$ in Eq. (19) the Poynting vector looks more and more like that of a single plane wave, traveling parallel to \mathbf{v}_g , with only a very slight periodic modulation superimposed on it. For $\alpha=0$ however, the modulation is 100%, and \mathbf{v}_g points parallel to the grating lines.

IV. INTERFERENCE OF TWO FLOQUET-BLOCH WAVES

Three general conditions are required for interference to occur. The two waves first have to *overlap* in space. In the case of two finite Floquet-Bloch beams, the points of launching and the directions of the group velocities must allow this to occur. Secondly, there must be a relative difference in the lengths or directions of the wave vectors of the two Floquet-Bloch waves. This ensures that spatial beats will occur. And thirdly, the polarization states of the two Floquet-Bloch waves must be nonorthogonal. But are these three conditions sufficient for the observation of visible fringes? The answer is no, not necessarily, for there are in addition two classes of Floquet-Bloch wave interference, which I shall designate *normal* (real fringes) and *exchange* (virtual fringes). Pure normal interference implies redistribution of energy in real space, *without* any change in the angular energy distribution of the field. Pure exchange interference implies no redistribution of energy in real space, but instead its angular distribution changes, energy getting *exchanged* between the (0) and (-1) groups of spectral plane waves. Assuming that light in a corrugated planar waveguide gets scattered out of the guide plane in an isotropic scalar manner (i.e., proportional to the local intensity, independently of the orientation of the phase velocity and the polarization of the light), pure normal fringes will be visible, and pure exchange fringes invisible. However, as I will now show, mixed cases can also occur, exhibiting elements of both types of interference. In the discussion the influence of the polarization is not considered, the electric fields of the two Floquet-Bloch waves being taken as having scalar amplitudes. This point will be further considered in Sec. V.

A. Notation

The two interfering Floquet-Bloch waves are labeled with superscripts 0 and 1 in front of their parameters. Scaling their normalized mode shapes with the real-valued field constants 0E and 1E , the total electric field is

$$\mathbf{E}(\mathbf{r}) = \hat{\mathbf{z}} \sum_{m=0}^1 \sum_{n=-1}^0 {}^m E {}^m V_n \exp(-j {}^m \mathbf{k}_n \cdot \mathbf{r}). \quad (20)$$

The tie points of two Floquet-Bloch waves are shown for one particular case on the stop-band branches in Fig. 2. The orientation and spacing of the coarsest fringes that can occur is given by the shortest wave-vector difference that exists on the wave-vector diagram, that is, the wave vector δ between these two tie points

$$\delta = ({}^0 \mathbf{k}_0 - {}^1 \mathbf{k}_0) = ({}^0 \mathbf{k}_{-1} - {}^1 \mathbf{k}_{-1}). \quad (21)$$

The spacing of the fringes is then $2\pi/|\delta|$ and they will be oriented normal to δ . In terms of the coordinates ξ and η , δ can also be written

$$\delta = [({}^0 \xi - {}^1 \xi) \hat{\mathbf{x}} + ({}^0 \eta - {}^1 \eta) \hat{\mathbf{y}}] \quad (22)$$

and the slant angle γ between the fringes and the x axis can then easily be shown to be

$$\tan \gamma = - \left[\frac{{}^0 \xi^\dagger - {}^1 \xi^\dagger}{{}^0 \eta^\dagger - {}^1 \eta^\dagger} \right] \tan \theta_B, \quad (23)$$

where normalized versions of ξ and η have been used [see Eq. (16)].

B. Normal interference

To test for the presence of real coarse interference fringes, one simply takes the modulus squared of the field amplitude in Eq. (20), and retains only the constant and slowest-varying terms (i.e., those with spatial periods equal to $2\pi/|\delta|$). The resulting intensity distribution is

$$I(\mathbf{r}) = {}^0 E^2 + {}^1 E^2 + 2 {}^0 E {}^1 E ({}^0 V_0 {}^1 V_0 + {}^0 V_{-1} {}^1 V_{-1}) \cos(\delta \cdot \mathbf{r}) \quad (24)$$

yielding a normal visibility v_N of

$$v_N = \frac{2 {}^0 E {}^1 E}{{}^0 E^2 + {}^1 E^2} ({}^0 V_0 {}^1 V_0 + {}^0 V_{-1} {}^1 V_{-1}). \quad (25)$$

In deriving Eqs. (24) and (25), the fact that the mode shapes in Eq. (18) are normalized has been used. This visibility is the product of something that looks like the conventional visibility of two interfering plane waves times a term involving the mode shapes of the Floquet-Bloch waves. A condition exists for v_N to be zero, without either ${}^0 E$ or ${}^1 E$ being zero. This is

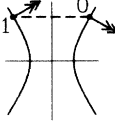
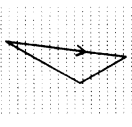
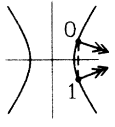
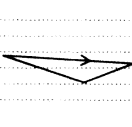

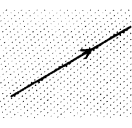
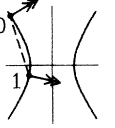
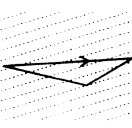
$$\frac{{}^0 V_0 {}^1 V_0}{{}^0 V_{-1} {}^1 V_{-1}} = -1. \quad (26)$$

From Eqs. (18) and (26), it is easy to show that $v_N=0$ if the tie points are on opposite branches of the stop band with equal η coordinates, i.e., if

$$\begin{aligned} {}^0 \eta^\dagger &= {}^1 \eta^\dagger, \\ {}^0 \xi^\dagger &= -{}^1 \xi^\dagger. \end{aligned} \quad (27)$$

This is illustrated in Table I. What are the implications of this result? We have two waves of nonzero amplitudes and different phase velocities that do not produce any real

TABLE I. Chart of various types of Floquet-Bloch wave interference. The total spatially averaged Poynting vector $\langle \mathbf{S}_{av} \rangle$ of the superposition of two Floquet-Bloch waves is found by adding together their average Poynting vectors (these lie parallel to their group velocities). The fringe spacing is inversely proportional to the length of the difference wave vector between the two tie points.

	Tie points	Fringes and $\langle \mathbf{S}_{av} \rangle$	${}^0E/{}^1E$	v_E	v_N
(a)			1 $\neq 1$	$1/[(1+\eta^\dagger)^2]^{1/2}$ $\neq 0$	0 0
(b)			1 $\neq 1$	0 $\neq 0$	$(1/\xi^\dagger)$ $\neq 0$
(c)			1 $\neq 1$	$(1/\xi^\dagger)^2$ $\neq 0$	$-[1-(1/\xi^\dagger)^2]^{1/2}$ $\neq 0$
(d)			$(1+{}^0\eta^{\dagger 2}/1+{}^1\eta^{\dagger 2})^{1/2}$ otherwise	0 $\neq 0$	$\neq 0$ $\neq 0$

interference fringes. To understand how they interact, we need to discuss exchange interference.

C. Exchange interference

One can gain an interesting insight into the reasons for exchange interference by considering power conservation. First we need to derive the Poynting vector of the superposition of two Floquet-Bloch waves in Eq. (20). It takes the form

$$\langle \mathbf{S}(\mathbf{r}) \rangle = \langle {}^0\mathbf{S}_{av} \rangle + \langle {}^1\mathbf{S}_{av} \rangle + \langle \mathbf{S}_m(\mathbf{r}) \rangle, \quad (28)$$

where

$$\begin{aligned} \langle \mathbf{S}_m(\mathbf{r}) \rangle = & ({}^0E {}^1E / \omega \mu) ({}^0V_0 {}^1V_0 \bar{\mathbf{k}}_{LP_0} \\ & + {}^0V_{-1} {}^1V_{-1} \bar{\mathbf{k}}_{LP_{-1}}) \cos(\delta \cdot \mathbf{r}) \end{aligned} \quad (29)$$

and the first two terms in Eq. (28) are the spatially averaged Poynting vectors of the Floquet-Bloch waves. Equation (29) is the interference term. If it has a nonzero component parallel to δ then power *cannot be conserved*, because the total amount of power carried by the field would fluctuate from point to point. It can be shown, after a bit of tedious algebra that, within the approximations of the analysis, $\langle \mathbf{S}_m(\mathbf{r}) \rangle$ is always oriented perpen-

dicular to δ . Hence power is always conserved. Exchange interference, as the name suggests, involves the redistribution of energy between the (0) and the (-1) groups of spectral plane waves. The (0) and the (-1) groups in Eq. (20), taken alone, yield the following intensity distributions:

$$I_n = ({}^0E {}^0V_n)^2 + ({}^1E {}^1V_n)^2 + 2 {}^0E {}^1E {}^0V_n {}^1V_n \cos(\delta \cdot \mathbf{r}), \quad n = 0, -1. \quad (30)$$

Imagine now that it is possible to block out the scattering from the (0) or the (-1) group of spectral waves [this is sometimes possible in planar waveguides because of the different polarization states of the (0) and (-1) waves]. Blocking out the (0) waves will result in an intensity distribution I_{-1} with a certain visibility. If this visibility does not change when instead the (-1) waves are blocked, then we have pure normal interference. The visibility of the fringes is then unaffected by whether or not either group of spectral waves is blocked. If on the other hand it *is* affected, then there is an element of exchange interference. This condition is effectively a test of whether or not the angular spectrum of the (0) group has the same shape as (-1) group. The visibility of the exchange fringes is conveniently defined as half the difference between the visibility of the (0) and the (-1) fringes, and takes the form (after some manipulation)

$$v_E = {}^0E {}^1E \frac{({}^0V_{-1} {}^1V_0 - {}^0V_0 {}^1V_{-1})({}^0E {}^2V_{-1} {}^0V_0 - {}^1E {}^2V_{-1} {}^1V_0)}{[({}^0E {}^0V_0)^2 + ({}^1E {}^1V_0)^2][({}^0E {}^0V_{-1})^2 + ({}^1E {}^1V_{-1})^2]}. \quad (31)$$

Under what circumstances is v_E zero? The numerator equals zero if either

$${}^0V_0/{}^0V_{-1} = {}^1V_0/{}^1V_{-1} \quad (32)$$

or

$$({}^0E/{}^1E)^2 = {}^1V_{-1} {}^1V_0/{}^0V_{-1} {}^0V_0. \quad (33)$$

The first of these conditions represents the trivial case when the two Floquet-Bloch waves are identical. The second condition is rather subtle. It can be satisfied (a) only if the two Floquet-Bloch waves have tie points lying on the *same* stop-band branch—otherwise the term on the right-hand side will be negative (0E and 1E are *real* quantities); and (b) only if the component *normal* to the fringes (i.e., parallel to δ) of the total average Poynting vector $\langle \mathbf{S}_{av} \rangle (= \langle {}^0\mathbf{S}_{av} \rangle + \langle {}^1\mathbf{S}_{av} \rangle)$ is zero. From simple geometrical considerations, this can happen only if the two tie points lie on the same side of the stop band, confirming the statement made in (a). This is also in agreement with the discussion in the paragraph following Eq. (29); if there is a component of total averaged power flow across the fringes, then energy conservation dictates that the fringe type must be at least partly *virtual*, since otherwise the amount of energy carried across the fringes would vary from point to point, something that is impossible since no energy sinks or sources exist.

A number of special cases are outlined in Table I. The first case is that of Eq. (27), and produces pure exchange fringes regardless of the relative amplitudes of the Floquet-Bloch waves. Case (b), with

$$\begin{aligned} {}^0\eta^\dagger &= -{}^1\eta^\dagger, \\ {}^0\xi^\dagger &= {}^1\xi^\dagger \end{aligned} \quad (34)$$

will exhibit pure normal interference if $({}^0E/{}^1E)^2 = 1$ (otherwise there would be an element of exchange interference since the total averaged Poynting vector $\langle \mathbf{S}_{av} \rangle$ would have a component parallel to δ). Case (c), with antisymmetric tie points, is mixed:

$$\begin{aligned} {}^0\eta^\dagger &= -{}^1\eta^\dagger, \\ {}^0\xi^\dagger &= -{}^1\xi^\dagger. \end{aligned} \quad (35)$$

It always has a component of $\langle \mathbf{S}_{av} \rangle$ normal to the fringes, and hence will always exhibit elements of both exchange and normal interference. In case (d), there will always be an element of normal interference, but $v_E = 0$ is possible provided the amplitudes 0E and 1E are chosen correctly so that the component of $\langle \mathbf{S}_{av} \rangle$ normal to the fringes is zero. The condition that must be satisfied for this to occur is of course Eq. (33).

These results are fairly extraordinary in several respects. In case (b) we have two Floquet-Bloch waves with rays diverging at angles 2α ($0 < \alpha < \theta_B$) producing real spatial fringes with periods

$$\lambda_{\text{eff}}(2 \sin \theta_B / M)[(\tan \theta_B / \tan \alpha)^2 - 1]^{1/2} \quad (36)$$

and visibilities v_N of

$$v_N = [1 - (\tan \alpha / \tan \theta_B)^2]^{1/2}. \quad (37)$$

In a typical case, with a Bragg angle of 40° , a grating

strength M of 0.01, a λ_{eff} of 350 nm, and an angle α of 35° , the two Floquet-Bloch waves diverging at 70° will interfere to produce real fringes with a period of 29.7 μm and a visibility of 0.55. On the other hand, in case (c) one sees (at least within the approximations of the model) two *collinear* waves producing real fringes with a similar period.

V. EXPERIMENTAL RESULTS

Finally I want to present some new experimental results confirming the existence of both types of interference (some preliminary results are available in Ref. 8). The observations were made in corrugated Ta_2O_5 (refractive index 2.12) waveguides, formed by rf sputter deposition onto glass (refractive index 1.472) substrates. The guides were made single mode [supporting one transverse electric (TE), and one transverse magnetic (TM) mode⁹], the guiding layer being typically about 160 nm thick, and corrugations were rf sputter etched into them through holographic masks formed in photoresist. The grating period was set to around 300 nm, permitting Bragg angles in the region of 40° . The corrugated waveguides that resulted had losses of typically a few dB/cm. The analysis in the preceding sections is valid in outline, if not in detail, for the three different types of Bragg interaction that can occur in these guides, namely TE-TE, TE-TM, and TM-TM conversion. The differences are reflected in w_{SB} and κ , which will now depend on the polarization states of the two spectral waves (TE or TM), and hence on the Bragg angles.¹⁰ The exact form of this relationship does not concern us here, for it is possible to derive an accurate *effective* value of the modulation depth M from experimental measurements of the spacing between the interference fringes of the two Floquet-Bloch waves.

And strange though it may seem at first, the visibilities of the normal and exchange fringes discussed in the last section are essentially *unaffected* by the fact that the electric fields of the two guided modes in any particular integrated Floquet-Bloch wave are vector, not scalar, quantities. This is because the effect of polarization is implicitly present in the magnitude of the stop-band width w_{SB} . Should the state of polarization of the (0) group of spectral waves be orthogonal to that of the (-1) group, then w_{SB} will be zero, and no interference will occur.

A. Exchange interference

Exchange interference was observed in the situation depicted in Fig. 3, where a spatially narrow beam I (i.e., one with a wide angular line-wave spectrum) is incident "at the Bragg angle," i.e., its *central* line-wave satisfies the Bragg condition. On the left-hand side of the boundary the waveguide is smooth, so that the incident TM beam can be represented in wave-vector space (see the lower part of Fig. 3) by a small arc of the circle

$$\mathbf{k}_0^2 = (k_v N_{\text{TM}})^2,$$

where N_{TM} is the effective index of the TM modes. Requiring that components of phase velocity parallel to the boundary should be conserved leads to construction lines such as AA and BB ; the modal line-waves I_{AA} and I_{BB} of

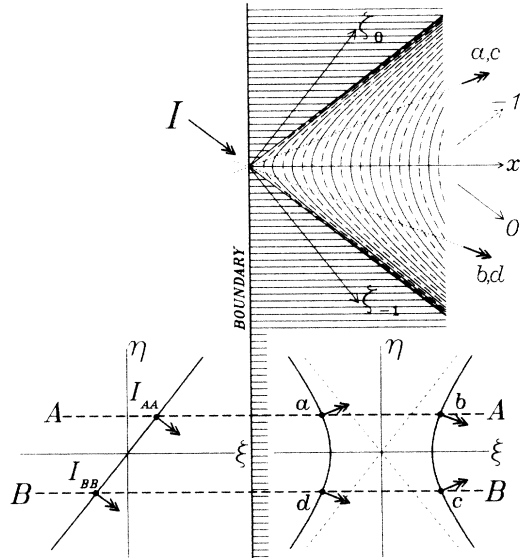


FIG. 3. Hook-shaped fringe pattern created by incidence of a narrow beam at the Bragg angle. Along the dotted and solid hyperbolas the energy in the light is carried predominantly by spectral waves progressing in phase in the (-1) and (0) directions, respectively. The horizontal lines represent the orientation of the grating, and the coordinate axes ξ_0 and ξ_{-1} are perpendicular to the upper and lower Bragg angles. The lower part of the figure contains the reciprocal-space representation of the light present on each side of the boundary, the group velocities (the ray directions) of the various Floquet-Bloch waves being given by the double-headed arrows. See the text of Sec. V A for more details.

the input spectrum each excite two Floquet-Bloch waves inside the corrugated region, with tie points a and b , and c and d , respectively. This is true for every spectral line-wave of the incident beam, and hence if the angular spread of the incident light is large enough, tie points all along both stop-band branches will get excited. The consequence in real space (see top part of Fig. 3) is that the light spreads out in the direction of the group velocities (indicated by double-headed arrows in the figures) over a fan-shaped region bounded by the upper and lower Bragg angles. In addition, interference will exist between pairs of spatially superimposed Floquet-Bloch waves such as a,c and b,d . The slant and period of the resulting fringes is given by the difference wave vector between the associated tie points. The fringe type will mostly be a mixture of exchange and normal, except at the waist of the stop band, where it will be purely exchange.

Experimental confirmation of Fig. 3 is shown in the sequence of photographs in Figs. 4–6, where a narrow TM beam is incident at the Bragg angle (38° in this case) for TM-TM conversion. First of all, in Fig. 4, no polarization filter was used, and the TM-polarized beam can be seen entering the corrugated region from the upper left, and spreading out over a fan-shaped region as predicted in Fig. 3. Notice that a significant proportion of the incident energy (i.e., that in the outer reaches of the angular spectrum, exciting Floquet-Bloch waves with tie points far from the stop-band center) travels through in the (0)

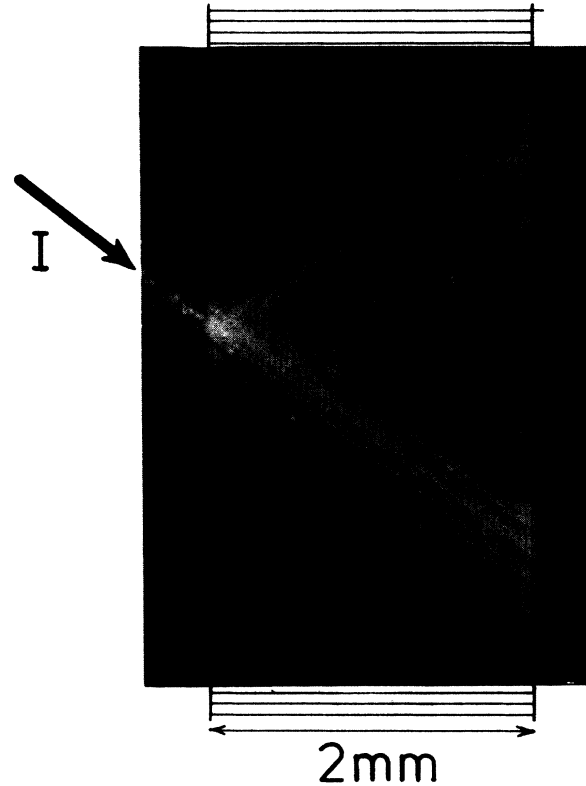


FIG. 4. Photograph of narrow TM beam entering a corrugated waveguide region at the Bragg angle for TM-TM conversion. No polarization filter was used. Notice way in which the light spreads out over a fan-shaped region, and the absence of any normal interference fringes along a line from the entry point parallel to the grating lines (the x axis in Fig. 3). The anomalous streak is caused by a grating imperfection. See the text for values of the experimental parameters.

direction without being affected by the grating. The presence of some normal interference is apparent, producing low-visibility hook-shaped fringes in regions above and below the x axis (refer to Fig. 3). Along the x axis, the visibility of these normal fringes is zero, as predicted for two Floquet-Bloch waves with tie points placed at equal η values on opposite sides of the stop band.

TM modes in these strongly guiding single-mode guides have a large component of electric field parallel to their propagation directions, in the plane of the guides. The other component of electric field (pointing normal to the guide plane) scatters only very weakly. Hence the light escaping out of the guide plane from the (0) group of spectral line-waves will have a polarization state almost orthogonal (depending on the Bragg angle) to that scattered by the (-1) group. The consequence here is that exchange fringes can be made visible if a polarization filter is used to block out the light scattered from either one of these groups.

In Fig. 5, the light scattered by the (0) spectral group is blocked out using a correctly oriented filter, and the visibility of the hook-shaped fringe set is greatly enhanced. This change in visibility points to the presence of strong exchange interference. Finally, in Fig. 6, light scattered from the (-1) spectral group is blocked out, and a set of

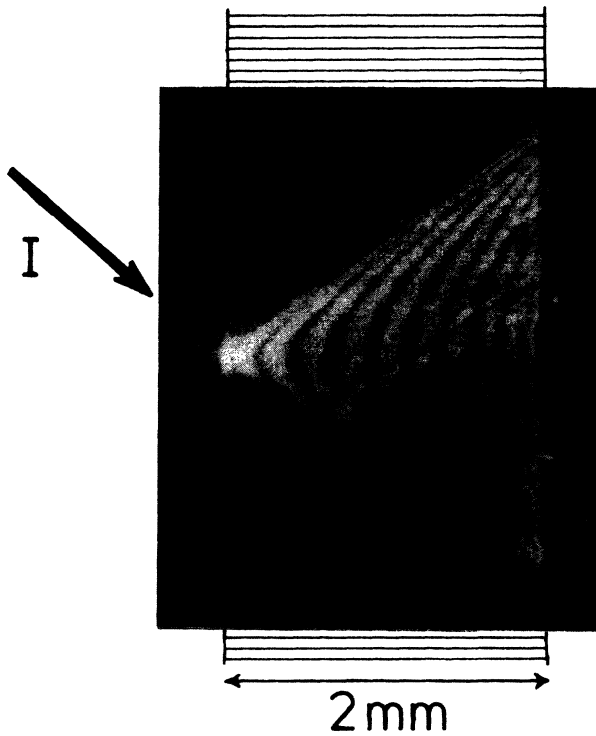


FIG. 5. The same situation as in Fig. 4, except that the light scattered from the (0) group of spectral line-waves was blocked using a correctly oriented polarization filter. Notice the strong exchange fringes that appear along the x axis.

exchange fringes complementary (i.e., shifted half a fringe spatially) to the previous set appears.

The absolute position of these fringes can be found using the methods of two-dimensional coupled-wave theory;¹¹ the bright fringes of the (0) group (drawn with solid lines in Fig. 3) occur along the hyperbolas

$$x^2 \sin^2 \theta_B - y^2 \cos^2 \theta_B = (z_n / \kappa)^2 \sin^2 2\theta_B, \quad (38)$$

where z_n is the n th zero of a *zeroth*-order Bessel function of the first kind. The bright fringes of the (-1) group (dashed lines in the figure) occur when z_n is the n th zero of a *first*-order Bessel function of the first kind. The parameters used to construct Fig. 3 were derived from the experimental results, and it can be seen that the correspondence is fairly good. The optical wavelength was 632.8 nm, and the grating period 310.5 nm, giving (for the Bragg angle of 38°) an average effective TM guide index inside the corrugated region of 1.655. The period of the exchange fringes along the x axis (parallel to the grating lines) was experimentally determined to be 0.199 mm (width of corrugated region is 2 mm), yielding a coupling constant κ of 12.44 mm⁻¹. If a hyperbolic output boundary is fabricated, lying exactly over one of these bright fringes, then a wide Bragg-reflected beam will leave the corrugated region. One will obtain an efficient beam expander, the inversion of the beam *squeezer* reported previously.⁴

Finally here I would like to point out that the system of hook-shaped fringes in Fig. 3 is a picture of a two-

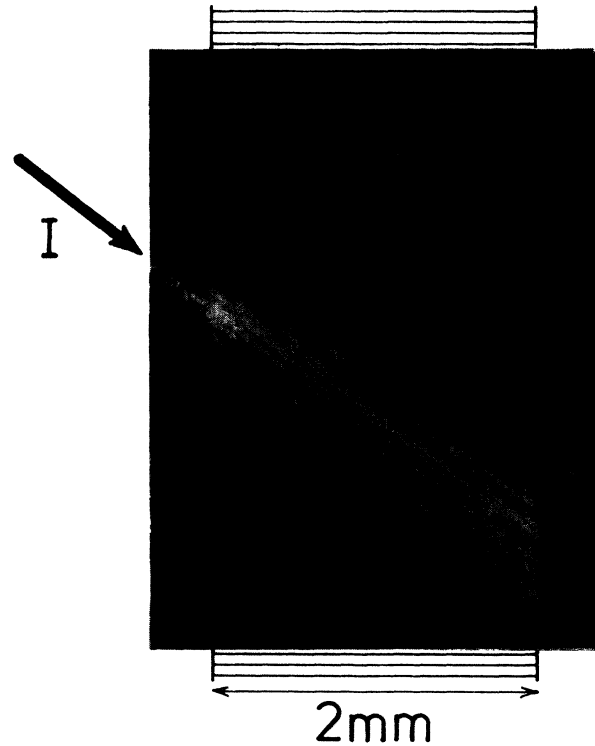


FIG. 6. The same situation as in Fig. 5, with the light scattered from the (-1) group of spectral line-waves blocked using a correctly oriented polarization filter. Notice the strong exchange fringes (complementary to those in Fig. 5) that are visible along the x axis. This photograph, together with the one in Fig. 5, was used as the basis of the hook-shaped fringe system drawn in Fig. 3.

dimensional Green's function, yielding the influence of a point excitation (I in this case) at the boundary on the field amplitude at an arbitrary point inside the corrugated region. The "point" in this case must be created by a diffraction-limited beam with an angular spectral width much greater than $2w_{SB}/Nk_v \sin \theta_B$, so that a continuous spectrum of Floquet-Bloch waves with tie points all along the stop-band branches can emanate from the entrance point. Earlier evidence for this type of interference can be found in the realm of x-ray diffraction by perfect crystals,¹² although because of experimental constraints the fringes could not (unlike in the present case) be observed directly.

B. Normal interference

Strong normal interference can be observed when Floquet-Bloch waves get reflected at a boundary with a smooth waveguide (see Fig. 7). The incident and the reflected Floquet-Bloch waves are then able to overlap spatially, and since their tie points lie on the same stop-band branch, the resulting interference is predominantly normal. Notice that (in order to make possible direct comparison with the experimental photograph in Fig. 9) the sense of the x and ξ axes in Fig. 8 has been reversed. Once again a narrow beam is incident at the Bragg angle,

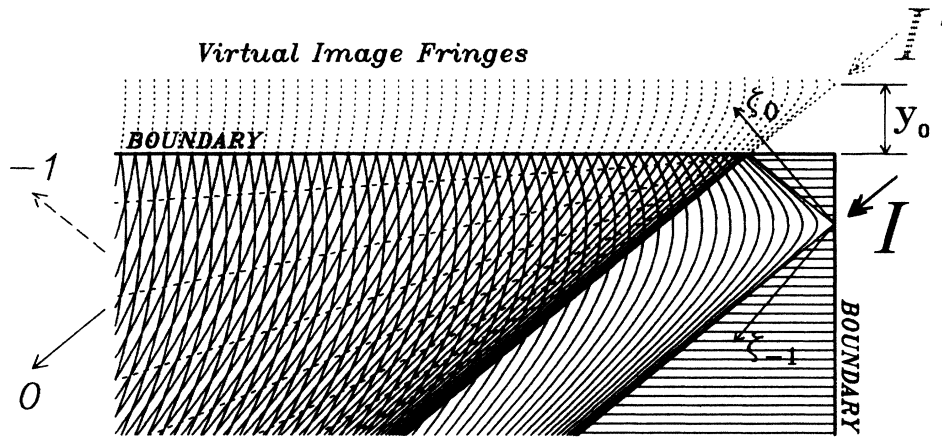


FIG. 7. Geometry used for the observing predominantly normal interference. For clarity, the hyperbolic loci of the antinodes of the (-1) group of spectral line-waves are omitted. The dashed lines sloping down and to the left follow the bright normal fringes that appear. See the text for more details.

and a spectrum of Floquet-Bloch waves spreads out over a triangular region. For clarity the loci of antinodes of the (-1) group of hyperbolic fringes are omitted. Upward-traveling Floquet-Bloch waves get reflected at the horizontal boundary, creating a set of reflected hook-shaped

fringes that appear to emanate from a virtual point source I' a distance y_0 behind the boundary. The result is an overlap region and (in the figure) a Moiré pattern whose beats define the position and orientation of a set of predominantly normal fringes. The situation is further

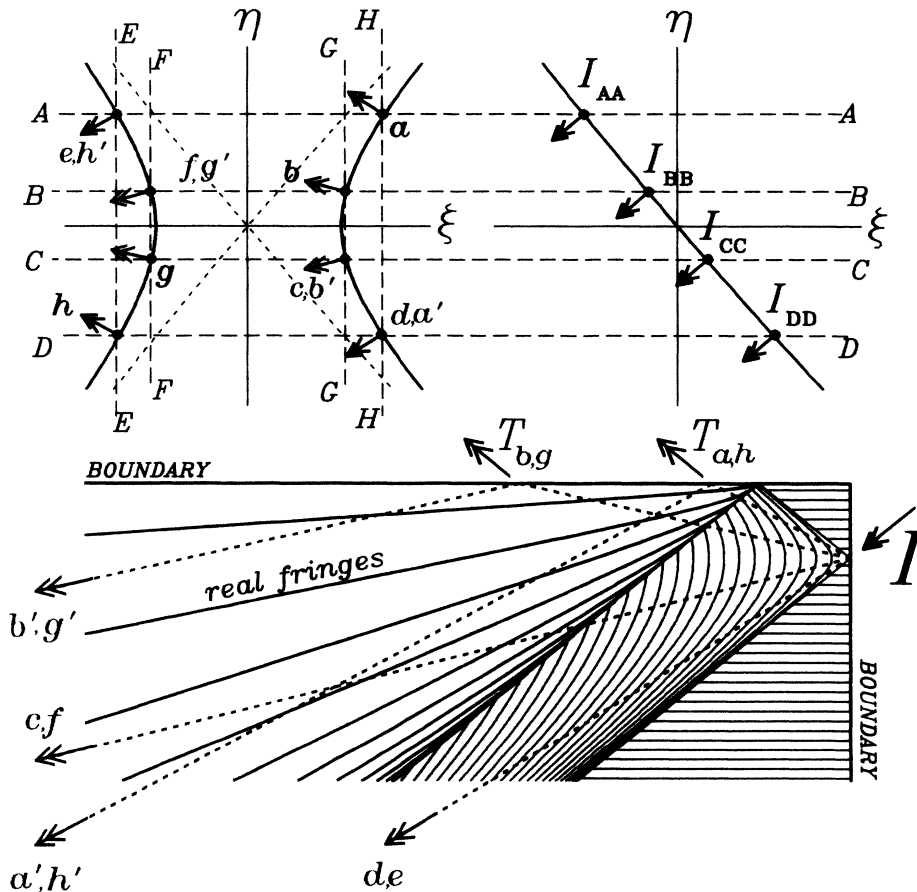


FIG. 8. Diagram explaining the complicated fringe structure in the overlap region in Fig. 7. The dotted lines represent the paths taken by the Floquet-Bloch rays. Predominantly real fringes (drawn in this time with solid lines and sloping downwards and to the left) are created where these lines intersect.

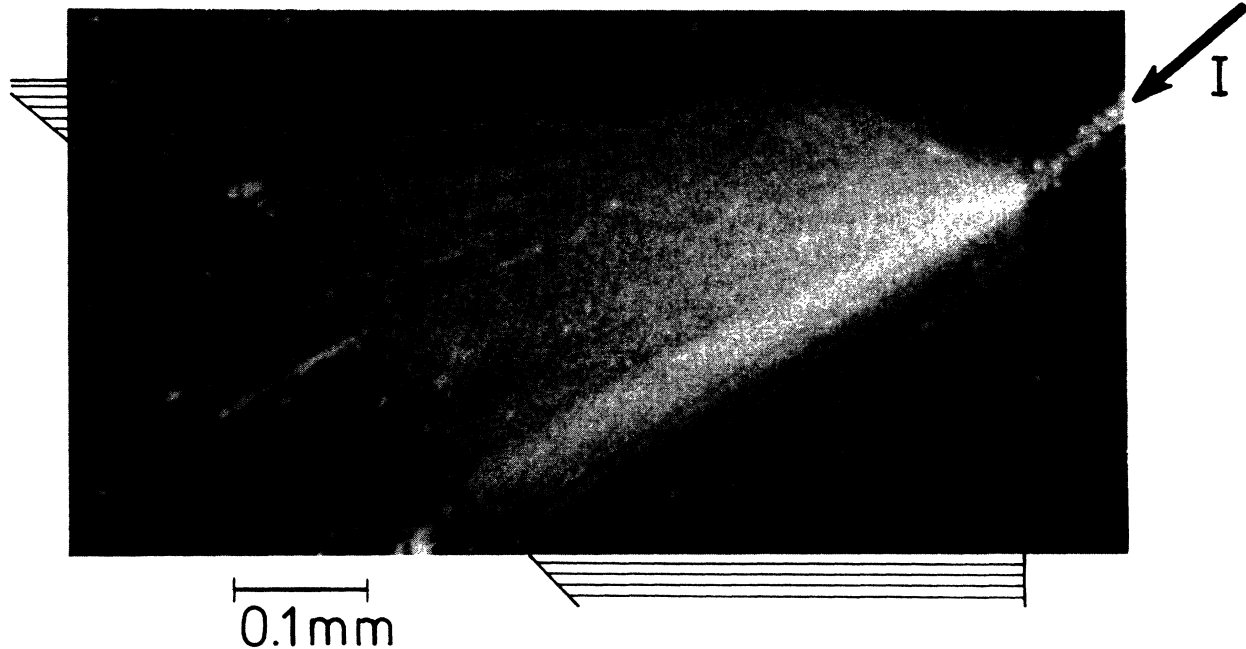


FIG. 9. Photograph used as the basis of Figs. 7 and 8. No polarization filter was used, and real fringes slanting upwards and to the right are clearly visible. The curving left-hand boundary is purely coincidental, and is of no significance in the present discussion. Also very faintly visible are a set of hook-shaped fringes similar to those in Figs. 5 and 6, although here they are finer, indicating that the grating is stronger. See the text for values of the experimental parameters.

explained in Fig. 8, where the paths taken by the Floquet-Bloch rays inside the overlapped region are drawn in, their directions having first been obtained from the wave-vector diagram. For example, the line-waves I_{AA} and I_{DD} of the input spectrum excite Floquet-Bloch waves with tie points a and e , and d and h , respectively, where phase-velocity matching parallel to the vertical boundary has once again been used to construct the lines AA and DD . The Floquet-Bloch waves with tie points a and h travel upwards towards the boundary, where they generate a transmitted line-wave $T_{a,h}$ in the smooth guide, and two reflected Floquet-Bloch waves with tie points a' and h' (identical to d and e). These reflected waves travel back into the grating along trajectories given by their group velocities. All along this path predominantly virtual hook-shaped fringes are generated. The spectral line-waves I_{BB} and I_{CC} yield construction lines BB and CC , and four Floquet-Bloch waves with tie points b and f , and c and g , respectively. The rays associated with tie points c and f cross the ray a',h' , and at that point interference occurs, with fringes whose orientation and period are given by the wave-vector difference between the two tie points c and a' (equal to that between f and h') on the wave-vector diagram. The same is true for Floquet-Bloch waves a',h' and b,g , and in fact at every point in the overlap region four intersecting Floquet-Bloch rays can be found. The result is a complicated lattice consisting of two intersecting nets of predominantly virtual hook-shaped fringes, and a set of predominantly real fringes that slant upwards and to the right.

The photograph in Fig. 9 was used as the basis of the plots in the previous two figures. The conversion was

TM-TM, the Bragg angle 40° , the wavelength 632.8 nm, the grating period 310.5 nm, $y_0=0.1$ mm, and the maximum exchange-fringe period was 0.02 mm. These values lead to an effective TM index of 1.585, a modulation depth $M=0.031$, and a coupling constant of 120.3 mm^{-1} . The slanted normal fringes are easily seen, and the correspondence with the previous two figures is convincing. Earlier experimental observations of normal interference can be found in the work of Uragami in x-ray diffraction.¹³

VI. CONCLUSIONS

Floquet-Bloch waves can interfere in two distinct ways, resulting in both visible (normal interference) and virtual (exchange interference) spatial fringes. The wave-vector diagram provides a powerful means of summarizing these two types of interference, and of deriving detailed analytical results concerning the visibility, orientation, and spacing of the resulting fringes. A very simple condition exists for testing for the presence of exchange interference. It is based on the requirement that the fields should conserve power, and turns on the necessity that the total averaged Poynting vector should have no component flowing across the fringes. Given the correct choice of tie points, and grating strengths that are realizable in practice, two *monochromatic* Floquet-Bloch waves with either (a) *collinear* ray paths, or (b) with ray paths diverging at angles of anything between a few degrees and $2\theta_B$, can produce real fringes with a spacing of some tens of micrometers. Experimental observation of integrated Floquet-Bloch waves in corrugated Ta_2O_5 waveguides gives one a way of

seeing the two types of interference directly, through the light scattered out-of-plane by ever-present and randomly distributed cosmetic imperfections in the guides. Photographs of the images created by this scattered light confirm the general theoretical results. The Floquet-Bloch approach, its usefulness substantially improved by the wave-vector diagram, is most elegant in leading to a complete description of all aspects of the behavior of light in periodically stratified media.

ACKNOWLEDGMENTS

I wish to express my gratitude for the financial support provided by the Alexander von Humboldt Foundation during the experimental phase of the work reported here, and also to thank Reinhard Ulrich for placing at my disposal the excellent facilities in his laboratory at the Technische Universität Hamburg-Harburg in Hamburg, West Germany.

¹R. S. Chu and T. Tamir, Proc. IEE (London) **119**, 797 (1972).

²P. St. J. Russell, Opt. Commun. **48**, 71 (1983).

³R. Ulrich and R. Zengerle, in *Technical Digest of the Topical Meeting on Integrated and Guided-Wave Optics, Incline Village, Nevada, 1980* (Optical Society of America, Washington, D.C., 1980), p. TuB1-1.

⁴P. St. J. Russell, Electron. Lett. **20**, 72 (1984).

⁵Z. Pinsker, *Dynamical Scattering of X-rays in Crystals* (Springer-Verlag, Berlin, 1978).

⁶B. W. Batterman and H. Cole, Rev. Mod. Phys. **36**, 681 (1964).

⁷H. Kogelnik, Bell Syst. Tech. J. **48**, 2909 (1969).

⁸R. S. Chu and T. Tamir, Electron. Lett. **7**, 410 (1971).

⁹See, for example, H. Kogelnik, in *Integrated Optics*, edited by T. Tamir (Springer-Verlag, Berlin, 1979).

¹⁰K. Wagatsuma, H. Sakaki, and S. Saito, IEEE J. Quant. Electron. **QE-15**, 632 (1979).

¹¹P. St. J. Russell and R. Ulrich, *Proceedings of the Second European Conference on Integrated Optics, Florence*, Vol. 227 of *IEE Conference Publications* (IEE, London, 1983), p.88.

¹²C. Malgrange and A. Authier, C. R. Acad. Sci. **261**, 3774 (1965).

¹³T. Uragami, J. Phys. Soc. Jpn. **31**, 1141 (1971).

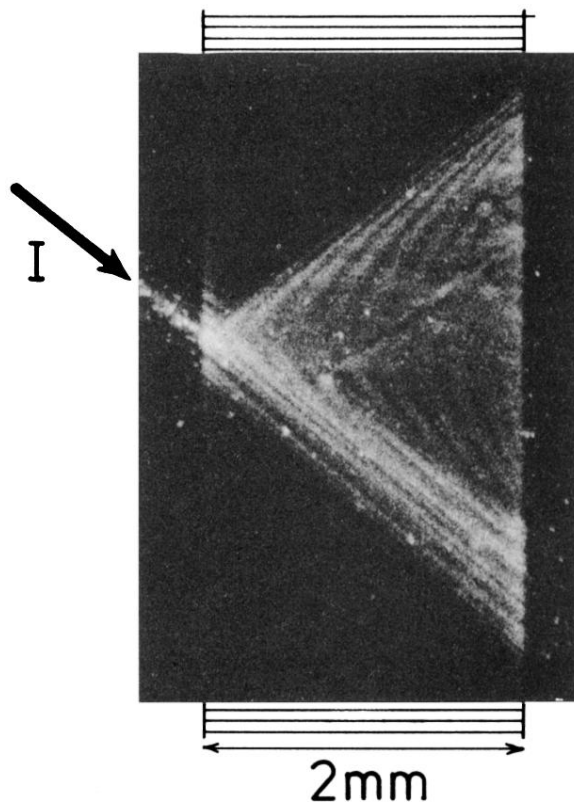


FIG. 4. Photograph of narrow TM beam entering a corrugated waveguide region at the Bragg angle for TM-TM conversion. No polarization filter was used. Notice way in which the light spreads out over a fan-shaped region, and the absence of any normal interference fringes along a line from the entry point parallel to the grating lines (the x axis in Fig. 3). The anomalous streak is caused by a grating imperfection. See the text for values of the experimental parameters.

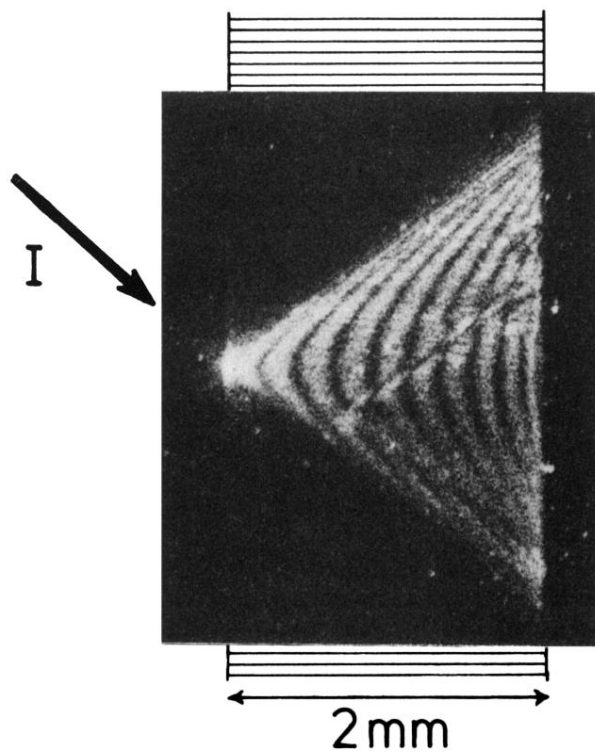


FIG. 5. The same situation as in Fig. 4, except that the light scattered from the (0) group of spectral line-waves was blocked using a correctly oriented polarization filter. Notice the strong exchange fringes that appear along the x axis.

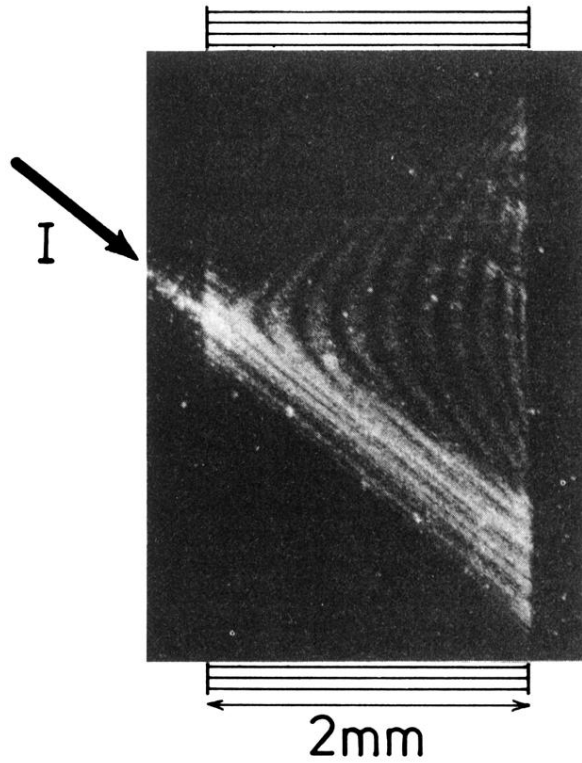


FIG. 6. The same situation as in Fig. 5, with the light scattered from the (-1) group of spectral line-waves blocked using a correctly oriented polarization filter. Notice the strong exchange fringes (complementary to those in Fig. 5) that are visible along the x axis. This photograph, together with the one in Fig. 5, was used as the basis of the hook-shaped fringe system drawn in Fig. 3.

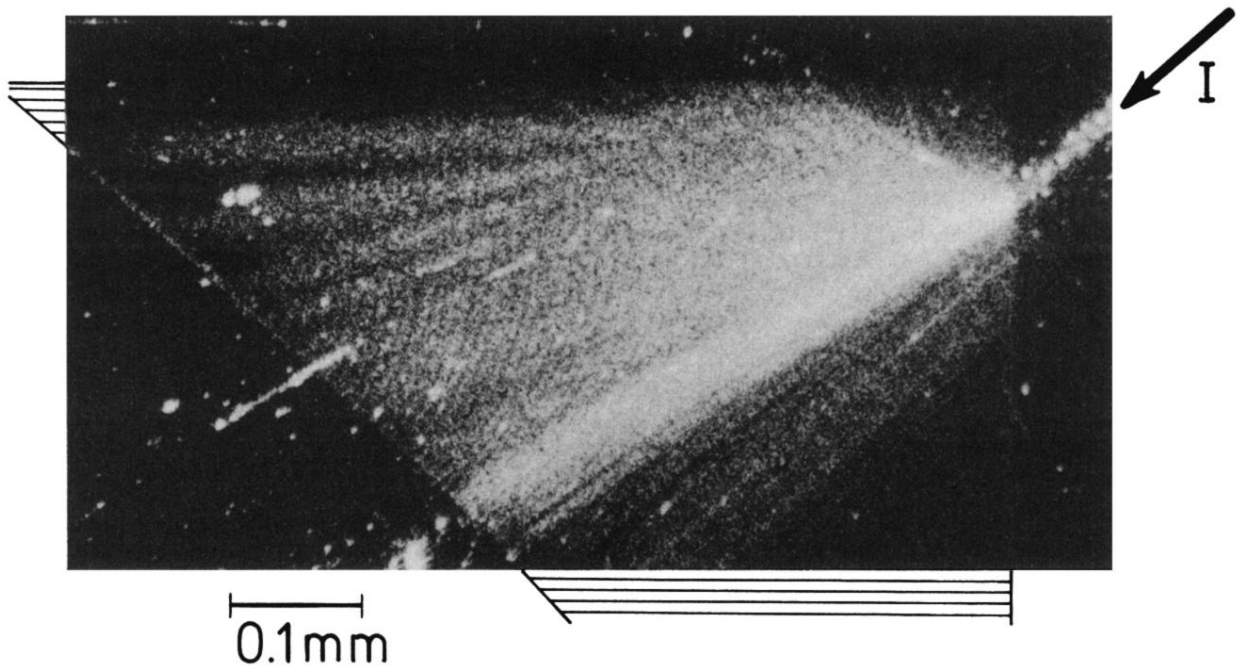


FIG. 9. Photograph used as the basis of Figs. 7 and 8. No polarization filter was used, and real fringes slanting upwards and to the right are clearly visible. The curving left-hand boundary is purely coincidental, and is of no significance in the present discussion. Also very faintly visible are a set of hook-shaped fringes similar to those in Figs. 5 and 6, although here they are finer, indicating that the grating is stronger. See the text for values of the experimental parameters.